

Chaotic Scenario in Three-Component Fermi Plasma

Tamal Ghosh¹, Suman Pramanick², Soumya Sarkar³, Ankita Dey⁴ and Swarniv Chandra^{5*}

¹*Department of Physics, Bidhannagar Govt. College, Kolkata, West Bengal 700064, India*

²*Department of Physics, Indian Institute of Technology Kharagpur, Kharagpur, West Bengal 721302, India*

³*Department of Physics, National Institute of Technology Karnataka, Karnataka 575025, India*

⁴*Department of Physics, Lady Brabourne College, Kolkata, West Bengal 700017, India*

⁵*Govt. General Degree College at Kushmandi, Dakshin Dinajpur, 733121, India*

**Institute of Natural Sciences and Applied Technology, Kolkata, India, 700032*

E-mail: tamalghosh695@gmail.com (corresponding author)

Electron Acoustic Solitary structures in Fermi Plasma with two temperature electrons have various applications in space and laboratory-made plasmas. Formulation of an adequate theory is important to understand various physical systems with various physical parameters. The motion of two temperature electrons in a quantum Fermi plasma system highly affects the solitary profile of the system. We study the quantum Fermi plasma system with two temperature electrons where the streaming velocities of two-electron population are opposite. We consider quantum hydrodynamic model (QHD) and derive a linear dispersion relation for the system. For non-linear study of the system, we use standard perturbative technique to derive Kortewegde Vries Burger's equation and show the evolution of solitary profile with different plasma parameters. We analyse the stable Rouge wave structure using NLSE and show simulation results. We study the dynamical properties and phase plot for two-stream quantum Fermi plasma system with two temperature electrons.

1. Introduction

Plasma systems containing two distinct groups of electrons show Electron-acoustic waves (EAWs). The distinction between two electron groups comes from their energy. Two types of electrons are 1) Hot electrons and 2) Cold electrons. The frequency of electron acoustic mode is higher than ion-acoustic frequencies of plasmas. Hot electrons can freely move with less viscous drag and supply restoring force, whereas cold electron feels viscous drag and produce inertia to the system. The thermal speed of hot electron is very large in comparison to cold electron. The phase speed of electron acoustic wave is smaller than the thermal speed of hot electrons but much larger than thermal speed of cold electrons. In this system ions may be considered as uniform neutralizing background. EAWs with two groups of electrons plays an important role in space plasma [1-4] as well as laboratory made plasmas [5-10]. The source of broadband electrostatic noises can be addressed with EAWs and it has been used to explain those. The wave emission in different regions of earth's atmosphere can be explained with EAWs. For these studies EAWs have become one of the important research areas in plasma physics.

In recent years there is a boost in the study of the nonlinear evolution of EAWs [11-14]. Various space-craft missions, e.g, the FAST at the auroral region [15-18] and the POLAR and GEOTAIL missions in the magnetosphere [19-21] explained by EAW related structures. Most of these application sites need theory and better understanding of non-relativistic classical plasmas. However, there are numbers of works on the theory of nonlinear propagation of electrostatic modes in quantum plasmas with consideration of quantum hydrodynamic model of plasma [22-27]. The non-linear wave structures of both cold and hot electrons are investigated [28, 29].

In this paper, we studied linear and nonlinear properties of EAWs in Fermi plasma with two temperature electrons. We first assumed basic hydrodynamic equations for the system then we normalized them using suitable scaling for the system. With the normalized equations on hand, we linearized them to get linear dispersion relation and linear dispersion characteristics are investigated. The Korteweg-de Vries Burgers (KdV-B) equation is derived using standard perturbation technique with taking only odd powers of perturbation fraction. We investigated dependence of soliton properties on different parameters of plasma. Then

we conclude the paper with some remarks and future work plans.

2. Basic Formulation

The plasma system that we considered is unmagnetized consisting of two groups of electrons. Two groups are (i) Hot electrons and (ii) Cold electrons. The thermal energy of hot electron is higher than cold electrons so the mobility of hot electron is large compared to that of cold electrons. So, in the momentum equation for hot electron we consider inertia term as zero, whereas in the momentum equation of cold electrons we consider a viscous term as its mobility is less and more responsive to the viscous forces.

2.1 Continuity equations

$$\frac{\partial}{\partial t}(\mathbf{n}_h) + \frac{\partial}{\partial x}(\mathbf{n}_h \cdot \mathbf{u}_h) = \mathbf{0} \quad (1)$$

$$\frac{\partial}{\partial t}(n_c) + \frac{\partial}{\partial x}(n_c \cdot u_c) = 0 \quad (2)$$

2.2 Momentum equations

$$0 = \frac{1}{m_e} \left[e \frac{\partial \phi}{\partial x} - \frac{1}{n_h} \frac{\partial P_h}{\partial x} + \frac{\hbar^2}{2m_e \gamma_h^2} \frac{\partial}{\partial x} \left(\frac{1}{\sqrt{n_h}} \frac{\partial^2 \sqrt{n_h}}{\partial x^2} \right) \right] \quad (3)$$

This is momentum equation for hot electrons. The inertia term (left hand side of the equation) is zero, as hot electrons are very mobile so its inertia can be assumed to be zero. Here, $\gamma_h = \frac{1}{\sqrt{1 - \frac{u_h^2}{c^2}}}$

$$\begin{aligned} & \left(\frac{\partial}{\partial t} + u_c \frac{\partial}{\partial x} \right) u_c \gamma_c \\ &= \frac{1}{m_e} \left[e \frac{\partial \phi}{\partial x} - \frac{1}{n_c} \frac{\partial P_c}{\partial x} + \frac{\hbar^2}{2m_e \gamma_c^2} \frac{\partial}{\partial x} \left(\frac{1}{\sqrt{n_c}} \frac{\partial^2 \sqrt{n_c}}{\partial x^2} \right) + \eta_c \frac{\partial^2 u_c}{\partial x^2} \right] \quad (4) \end{aligned}$$

This is momentum equation for cold electrons. The inertia term is non zero as the mobility of cold electrons is very less. For our two-electron plasma system cold electron produces the restoring force

for electron-acoustic oscillations. Cold electrons also got a viscous term. Here, $\gamma_c = \frac{1}{\sqrt{1 - \frac{u_c^2}{c^2}}}$

2.3 Poisson's equation

$$\frac{\partial^2 \phi}{\partial x^2} = 4\pi e(n_c + n_h - Z_i n_i) \quad (5)$$

The subscript i in the Poisson's equation is for representing ions. The above-mentioned equations are the governing equations for the plasma system, where n_h and n_c are the density of hot and cold electrons respectively. ϕ is the electrostatic potential. P_h is the pressure law for hot electrons. \hbar is the plank constant divided by 2π . m_e is the mass of electron and e is the charge of electron and η_c is the viscous constant for cold electrons.

2.4 The pressure law

We considered Fermi pressure as the main pressure component for electrons. Fermi pressure is

$$P_j = \frac{m_j V_{Fj}^2}{3n_{j0}^2} n_j^3 \quad (6)$$

Where, subscript $j = h$ is for hot electrons and $j = c$ for cold electrons. n_{h0} is the initial hot electron density.

The parameters need to be normalized to get a good control of the equations and normalized equations are easy to work with. Normalization means we need to define some suitable scaling associated with our problem. With these scaling constants we can make our parameters dimensionless.

For our problem, normalization has been done in following ways

$$\begin{aligned} x &\rightarrow \frac{x\omega_c}{V_{Fh}}; & t &\rightarrow t\omega_c; & \phi &\rightarrow \frac{e\phi}{2k_B T_{Fh}}; \\ n_h &\rightarrow \frac{n_h}{n_{h0}}; & n_c &\rightarrow \frac{n_c}{n_{c0}}; & u_h &\rightarrow \frac{u_h}{V_{Fh}}; \\ u_c &\rightarrow \frac{u_c}{V_{Fh}}; \end{aligned}$$

$$\text{Where, } \omega_c = \sqrt{\frac{4\pi n_{c0} e^2}{m_e}}; \quad V_{Fh} = \sqrt{\frac{2k_B T_{Fh}}{m_e}}$$

$$\text{and } H = \frac{\hbar\omega_e}{2k_B T_{Fe}}$$

Changing the variables and parameters accordingly we have Normalized Governing Equations.

$$\frac{\partial}{\partial t}(n_h) + \frac{\partial}{\partial x}(n_h \cdot u_h) = 0 \quad (7)$$

$$\frac{\partial}{\partial t}(n_c) + \frac{\partial}{\partial x}(n_c \cdot u_c) = 0 \quad (8)$$

$$0 = \frac{\partial \phi}{\partial x} - n_h \frac{\partial n_h}{\partial x} + \frac{H^2}{2\gamma_c^2} \frac{\partial}{\partial x} \left(\frac{1}{\sqrt{n_h}} \frac{\partial^2 \sqrt{n_h}}{\partial x^2} \right) \quad (9)$$

$$\begin{aligned} \left(\frac{\partial}{\partial t} + u_c \frac{\partial}{\partial x} \right) u_c \gamma_c &= \frac{\partial \phi}{\partial x} \\ &+ \frac{H^2}{2\gamma_c^2} \frac{\partial}{\partial x} \left(\frac{1}{\sqrt{n_c}} \frac{\partial^2 \sqrt{n_c}}{\partial x^2} \right) \\ &+ \eta_c \frac{\partial^2 u_c}{\partial x^2} \end{aligned} \quad (10)$$

$$\frac{\partial^2 \phi}{\partial x^2} = n_c + \frac{n_h}{\delta} - n_i \frac{\delta_1}{\delta} \quad (11)$$

Where, $\delta = \frac{n_{c0}}{n_{h0}}$ and $\delta_1 = Z_i \frac{n_{i0}}{n_{h0}}$

3. Linear Dispersion Relation

The system parameters can be expanded into following perturbation expansion for $n_h, n_c, u_h, u_c,$ and ϕ .

$$\begin{aligned} \begin{pmatrix} n_j \\ u_j \\ \phi \end{pmatrix} &= \begin{pmatrix} 1 \\ \pm u_{0j} \\ \phi_0 \end{pmatrix} + \epsilon^1 \begin{pmatrix} n_j^{(1)} \\ u_j^{(1)} \\ \phi^{(1)} \end{pmatrix} + \epsilon^2 \begin{pmatrix} n_j^{(2)} \\ u_j^{(2)} \\ \phi^{(2)} \end{pmatrix} \\ &+ \epsilon^3 \begin{pmatrix} n_j^{(3)} \\ u_j^{(3)} \\ \phi^{(3)} \end{pmatrix} + \dots \end{aligned} \quad (12)$$

Here we assume existence of streaming velocities for hot and cold electrons (+ve for hot electron and -ve for cold electrons) and equilibrium field in constant field ϕ_0 . Substituting these expansions in the governing relations and then taking only linear terms (linearizing) with the assumption that all field variable varies periodically as $e^{i(kx - \omega t)}$, we have following complex dispersion relation

$$\begin{aligned} -k^2 &= \frac{1}{\left[\frac{H^2 k^2}{4} \gamma_c^2 - \left(\frac{\omega - u_0 k}{k} \right)^2 \right] + i\eta_c (\omega - u_0 k)} \\ &+ \frac{1}{\delta} \frac{1}{1 + \frac{H^2 k^2}{4} \gamma_c^2} \end{aligned} \quad (13)$$

Here we assume $u_{0h} = u_{0c} = u_0$. Now we have to keep in mind that k itself is a complex number, $k = k_1 + ik_2$. Putting this into the expression of Complex dispersion relation we have two equations, one for real part of the equation and

other for imaginary part of the equation. The real dispersion equation is:

$$-1 = \frac{\left(\frac{1}{\delta} + k_1^2 + \frac{H^2 k_1^4}{4} \gamma_c^2 \right) \cdot \left[\frac{H^2 k_1^4}{4} \gamma_c^2 - \omega^2 - u_0^2 k_1^2 + 2\omega u_0 k_1 \right]}{\left[k_1^2 + \frac{H^2 k_1^2}{4} \gamma_c^2 \right]} \quad (14)$$

With $k_2 = 0$, if we plot ω vs k_1 then the plot will give us dispersion plot. H, u_0, δ are the parameters of the equation.

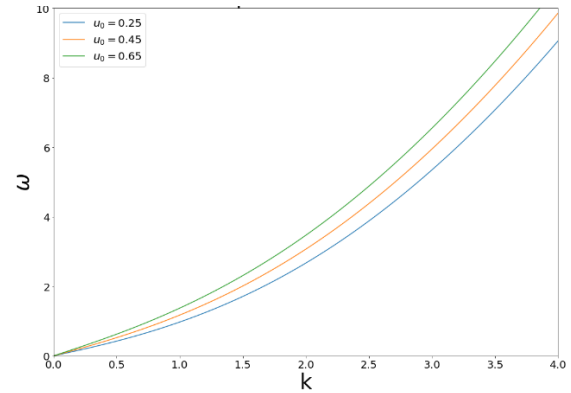


Fig.1: Dispersion relation plot for different u_0 keeping $\delta = 0.3$ and $H = 1$

Fig.1 shows dispersion plot for different values of equilibrium streaming velocity u_0 . Plot shows with increasing u_0 the slope of ω vs k plot increases, i.e. an increase in EAW velocity. Fig. 2. shows dispersion plot for different values of δ . Increase in δ shows decrease in slope (for small ω this behavior is clear). For $\delta = 1$ i.e. the density of hot and cold electrons are same, we are getting a linear behaviour in small k regime. Increasing delta means more initial cold electrons compare to hot electrons. So, according to our plots a greater number of initial cold electrons implies a decrease in k vs ω slop, that is increase in EAW velocity. Velocity of sound waves, rather acoustic waves increases with increasing the rigidity of the medium. Now a greater number of cold electrons mean more viscous drag and eventually more rigid medium, which can be the cause for an increase in EAW velocity. Fig.3. shows ω vs k plot for different H values. We change H from 1 to 3 keeping u_0, δ and constant. As H increases the slope of ω vs k plot increases that is also visible from the dispersion relation. However, H depends on plasma frequency ω_c linearly. So, higher H means higher plasma frequency. This leads to a

conclusion that for high plasma frequency the EAW has less wavenumber with same frequency.

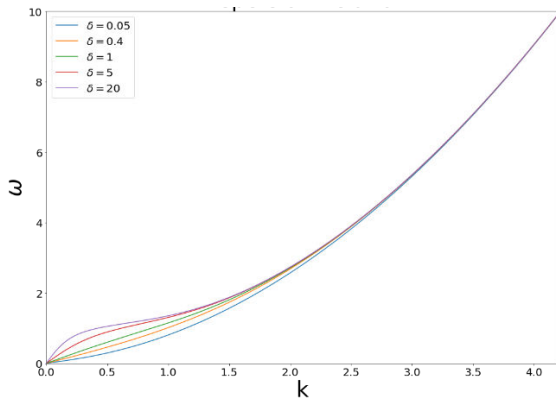


Fig.2: Dispersion relation plot for different δ keeping $u_0 = 0.25$ and $H = 1$.

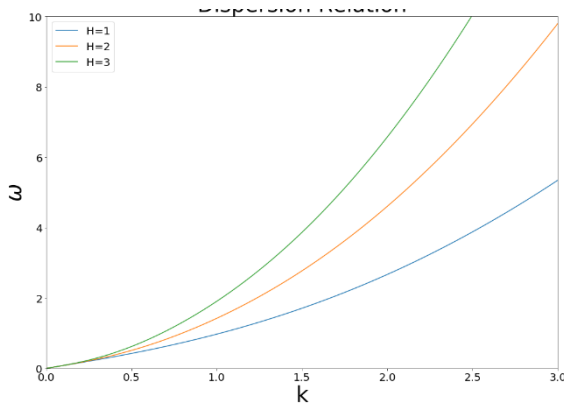


Fig.3: Dispersion relation plot for different H keeping $\delta = 0.3$ and $u_0 = 0.25$.

4. Korteweg-de Vries Burgers Equation for Nonlinear Study

We used standard reductive perturbation technique with usual stretching of space and time variables. We used two perturbation expansions to see the behavior of the solution of KdV-B equation. Using the perturbation expansion eq. (12) and, stretching of variables

$$\xi = \epsilon^{\frac{1}{2}}(x - v_0 t); \quad \eta = \eta_0 \epsilon^{\frac{1}{2}}; \quad \text{and} \quad \tau = \epsilon^{\frac{3}{2}} t \quad (15)$$

Putting them into governing equations and taking the lower order terms with power of epsilon we have the following KdV-Burger equation

$$\frac{\partial \phi}{\partial \tau} + A \phi \frac{\partial \phi}{\partial \xi} + B \frac{\partial^3 \phi}{\partial \xi^3} - C \frac{\partial^2 \phi}{\partial \xi^2} = 0 \quad (16)$$

The solution to (16) is

$$\phi = \frac{12D}{N} \text{sech}^2 \xi - \frac{36R}{15N} \tanh \xi$$

with,

$$A = \frac{2DS_1 R_1 + F n_{0c} R_1^2 - D(M - u_{0c}) \frac{Q_1^2}{n_{0h} \delta}}{DS_1 + n_{0c} R_1 \left(1 + \frac{3u_{0c}^2}{2c^2}\right)} \quad (17)$$

$$B = \frac{\left(D(M - u_{0c}) \left(\frac{T_h Q_1}{n_{0h} \delta}\right) - T_c S_1 n_{0c} - D(M - u_{0c})\right)}{DS_1 + n_{0c} R_1 \left(1 + \frac{3u_{0c}^2}{2c^2}\right)}$$

(18)

$$C = \eta_c R_1 \quad (19)$$

With,

$$D = M + \frac{3Mu_{0c}^2}{2c^2} - \frac{3u_{0c}^3}{2c^2} - u_{0c} \quad (20)$$

$$F = 1 + \frac{9u_{0c}^2}{2c^2} - \frac{3Mu_{0c}}{c^2} \quad (21)$$

$$T_c = \frac{H^2}{4n_{0c}^2} \left(1 - \frac{u_{0c}^2}{c^2}\right) \quad (22)$$

$$T_h = \frac{H^2}{4n_{0h}^2} \left(1 - \frac{u_{0h}^2}{c^2}\right) \quad (23)$$

$$S_1 = \frac{n_{0c}}{(M - u_{0c}) \left[\left(u_{0c} + \frac{3u_{0c}^3}{2c^2}\right) - M \left(1 + \frac{3u_{0c}^2}{2c^2}\right) \right]} \quad (24)$$

$$R_1 = \frac{1}{\left(u_{0c} + \frac{3u_{0c}^3}{2c^2}\right) - M \left(1 + \frac{3u_{0c}^2}{2c^2}\right)} \quad (25)$$

$$Q_1 = \frac{1}{n_{0h}} \quad (26)$$

For, $n_{0j} = 1$; $u_{0j} = 0$; $j = hc$

$$S_1 = -\frac{1}{M^2}; \quad R_1 = -\frac{1}{M}; \quad Q_1 = 1; \quad D = M; \quad F = 1;$$

$$T = \frac{H^2}{4}$$

Then, the values of the coefficients are:

$$A = \left(\frac{M^3}{2\delta} - \frac{3}{2M}\right) \quad (27)$$

$$B = \left(\frac{H^2}{8M} + \frac{M^3}{3} - \frac{M^3 H^2}{4\delta}\right) \quad (28)$$

$$C = -\frac{\eta_0}{M} \quad (29)$$

4.1 Solitary Profiles

Fig.4 shows an increase in the peak of the solitary profile with increasing H . For this plot $u_0 = 0.5$ and $\delta = 0.45$. Fig.6 show decrease in the peak of the

solitary profile with increasing δ . For this plot $u_0 = 0.5$ and $H = 2$

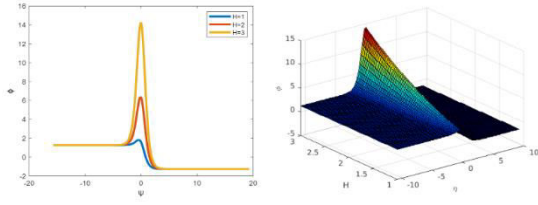


Fig.4: Solitary profile for different H keeping δ and u_0 constant. Left panel shows a 2D plot where right panel shows a 3D plot for the same.

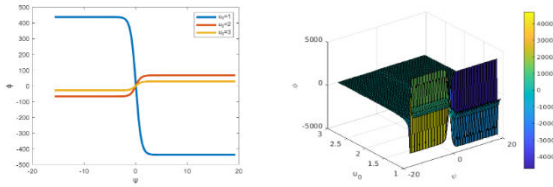


Fig.5: Solitary profile for different u_0 keeping δ and H constant. Left panel shows a 2D plot where right panel shows a 3D plot for the same.

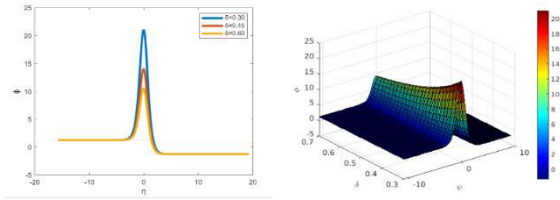


Fig.6: Solitary profile for different δ keeping H and u_0 constant. Left panel shows a 2D plot where right panel shows a 3D plot for the same.

5. Rogue Wave

KDV-B equation gives the solitary wave structures which are created due to the balance between the dispersive force and non-linear force in plasma. In case the balance breaks the KDV-B starts to modify itself to a sudden wave having amplitude almost twice or greater than the amplitude of normal waves at that time. Like the sudden high amplitude, the suddenness of its timing makes it more dangerous. The study of the Rogue wave is important as the interference of the waves from different directions and the non-linear property make it unpredictable. We study the stability of

Rogue wave and its evolution from our KDV-B equation

$$F = \epsilon^2 F_0 + \sum_{s=1}^{\infty} \epsilon_s (F_s e^{is\psi} + F_s^* e^{-is\psi}) \quad (30)$$

Where, F is the field variable, ϵ is the smallness parameter, and ψ is the phase factor. Now, using this equation we can expand the field variable i.e. the potential in KdV-B equation

$$\phi = \epsilon^2 \phi_0 + \epsilon \phi_1 e^{i\psi} + \epsilon \phi_1^* e^{-i\psi} + \epsilon^2 \phi_2 e^{2i\psi} + \epsilon^2 \phi_2^* e^{-2i\psi} + \dots \quad (31)$$

The first harmonics (ϕ_1) and second harmonics (ϕ_2) can be

$$\phi_1 = \phi_1^{(1)} + \epsilon \phi_1^{(2)} + \epsilon^2 \phi_1^{(3)} + \dots \quad \text{further}$$

$$\phi_2 = \phi_2^{(1)} + \epsilon \phi_2^{(2)} + \epsilon^2 \phi_2^{(3)} + \dots$$

expanded respectively

$$(32)$$

F_0 and F_s are assumed to vary very slowly with space and time. Now, we use the change in variables $\frac{\partial}{\partial \tau} = -is\omega - \epsilon c \frac{\partial}{\partial \rho} + \epsilon^2 \frac{\partial}{\partial \theta}$

$$(33)$$

$$\frac{\partial}{\partial \xi} = isk + \epsilon \frac{\partial}{\partial \rho} \quad \text{and put it in the equation}$$

and equate the coefficients of the first order of, we get

$$\omega = -Bk^3 \quad (34)$$

$$\frac{d\omega}{dk} = -3Bk^2 \quad (35)$$

Equating the coefficients of $e^{2i\psi}$ we have

$$\varphi_2^{(1)} = \frac{A}{6Bk^2} \varphi_1^{(1)2} \quad (36)$$

Equating the terms independent of ψ we have

$$\varphi_0^{(1)} = \frac{A}{C} \varphi_1^{(1)} \varphi_1^{(1)*} \quad (37)$$

By equating the other higher terms, we get

$$i \frac{\partial \varphi_1^{(1)}}{\partial \tau} + 3ikB \frac{\partial^2 \varphi_1^{(1)}}{\partial \rho^2} = -iAk \left(\varphi_1^{(1)} \varphi_1^{(1)} + \varphi_2^{(1)} \varphi_1^{(1)*} \right) \quad (38)$$

$$i \frac{\partial \varphi_1^{(1)}}{\partial \tau} - 3kB \frac{\partial^2 \varphi_1^{(1)}}{\partial \rho^2} + \frac{A^2}{6Bk} \left(\varphi_1^{(1)2} \varphi_1^{(1)*} \right) = 0 \quad (39)$$

Let's assume $P = ic - 3Bk$ and $Q = A^2k \left[\frac{1}{6Bk^2 + 4ikc} - \frac{1}{3Bk^2} \right]$. The term PQ is very important in defining the existence of a rogue wave. In the region $PQ < 0$ the rogue wave is stable and for $PQ > 0$ the rogue wave doesn't exist. We get the solution of Eq. (39) as

$$\phi(\rho, \theta) = \sqrt{\frac{2P}{Q}} \left[\frac{4(1 + 4iPQ)}{1 + 16P^2Q^2 + 4\rho^2} - 1 \right] \exp(2iP\theta) \quad (40)$$

Where, by changing the variables ρ and θ we get the rogue wave structure for a very short range of those variables and the amplitude is much larger than that of normal waves.

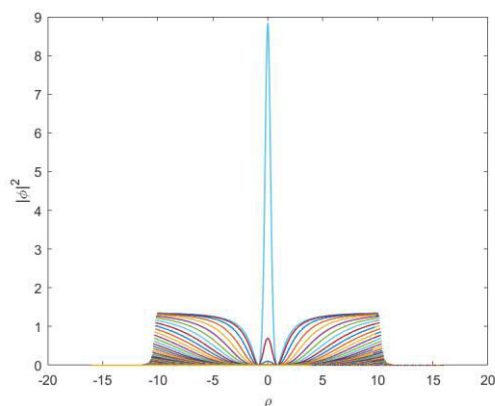


Fig.7: Rogue wave structure

In Fig.7 we plot the potential amplitude with the changed variable ρ for different values of θ . And we take almost 500 values of θ and as one can see that for only one value the potential suddenly gets abnormally high with respect to the other. All of the solutions we get from the same NLSE, where only one wave behaves dangerously. It perfectly depicts the feature of a Rogue Wave - the amplitude is way higher than that of solitary profiles in Fig. (4), Fig. (5), and Fig. (6).

Here we take the viscosity coefficient 5 and observed that the amplitude of the rogue wave in the plot is lower than that of the rogue wave with no viscous term.

6. Simulation of KdV-B and Rouge wave evolution

Here, in this section, we show the static plots of two simulations of the solitary profiles and rogue wave profile of the relativistic plasma we are working on. A movie of KdV-B evolution simulated with our codes can be found in this link: <https://doi.org/10.5281/zenodo.4366748> and a movie of Rouge wave evolution can be found in this link: <https://doi.org/10.5281/zenodo.4384499>.

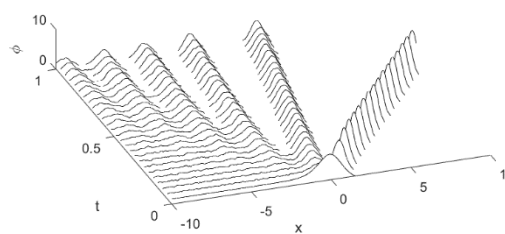


Fig.8: Simulation result of evolution of solitary profile.

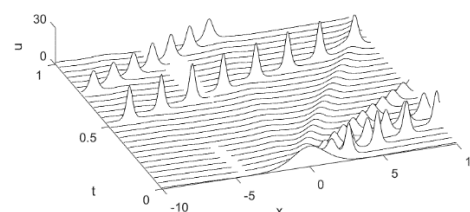


Fig.9: Simulation result of evolution of Rouge wave profiles.

In both figures, using the solutions of KdV-B and rouge wave, we simulate the KdV-B solitary wave and rogue wave respectively. Here, 'x' represents the space coordinate and 't' represents the time coordinate, and 'u' is the amplitude. In both cases, we see the changes in the waves in the interval between $t = 0s$ and $t = 1s$. As you can see from the simulations that rogue waves have much higher

amplitudes than those of normal solitary waves and also less frequent than normal waves.

7. Dynamical Study

To get the phase diagram of EAWs, we study a travelling wave solution followed by the KDV-B equation. To do that we use the transformation $\eta = \xi - M\tau$ with the proper boundary conditions at $\eta \rightarrow \pm\infty$, $\psi, \delta\psi/\delta\eta$ and $(\delta^2\psi)/(\delta\eta^2) \rightarrow 0$ where M is the velocity of the wave.

Applying a transformation like [30], we can write the Non-linear Schrodinger equation as

$$\frac{d^2\psi}{d\eta^2} = \left(\beta^2 - \frac{1}{M_1 l^2} \beta V\right) \psi - \frac{M_2}{M_1 l^2} \psi^3 \quad (41)$$

Eq. (41) can be written in the following dynamical form

$$\frac{d\psi}{d\eta} = z \quad (42)$$

$$\frac{dz}{d\eta} = M_1 \psi - M_2 \psi^3 \quad (43)$$

The phase plot gives the dynamical nature of the system (Fig.10). The progressive nature of EAW can be seen from Fig.11. Plot shows a stable solution. Different coloured plots in phase diagram correspond to different energy solutions. Green one is the highest energy and blue one is the lowest.

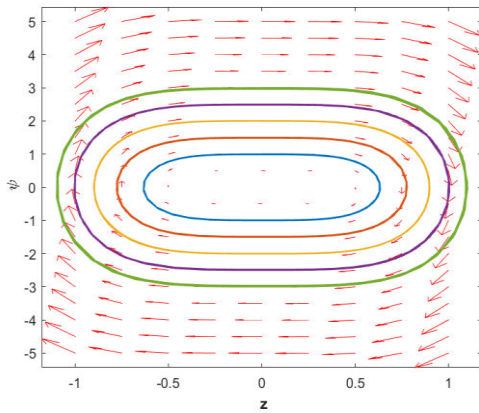


Fig.10: ψ vs z plot (Phase plot) for dynamical behaviour.

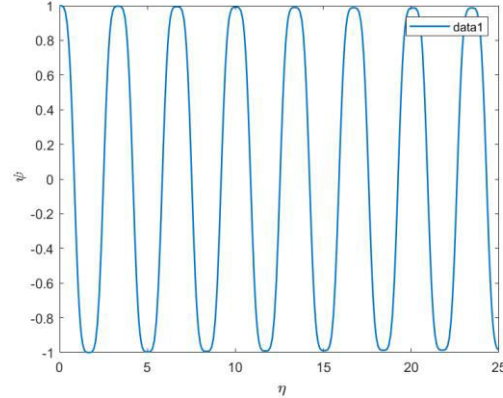


Fig.11: ψ vs η plot for dynamical behaviour.

8. Conclusion

Both the linear and nonlinear properties of electron-acoustic wave (EAWs) have been investigated in three component Fermi plasma consisting of two distinct groups of electrons and solitary ions. Dispersion relation that we obtained, is a general one including inertia effect for cold electrons and effect of Fermi pressure for hot electrons. The stable models for EAWs are shown. The dependence of electron-acoustic wave velocity on different plasma parameters is shown and explained.

The slope of the dispersion relation plots depends on the velocity of EAW inversely. The dependence of this EAW velocity and EAW frequency on different plasma parameters has been shown. Electron-acoustic wave velocity increases with increasing H , u_0 and δ and decreases with increasing viscous coefficient η_c . The formation of rouge wave in the system has been studied. The evolution of solitary profile and rouge wave has been studied. Dynamical properties of the system has also been studied and found a stable dynamical structure.

Acknowledgements

SP would like to acknowledge the support of institute fellowship by IIT Kharagpur and the scholarship provided by DST-INSPIRE. SC would like to thank the Institute of Natural Sciences and Applied Technology, the Physics departments of

Jadavpur University and Government General Degree College at Kushmandi for providing facilities to carry this work. The authors would like to thank the reviewers for their valuable inputs towards upgrading the paper.

References

- [1] Z. P. Ang. L.K., “,” *Phys. Rev. Lett.*, vol. 98, no. 164802, p. 187, 2007.
- [2] W. L. Barnes, A. Dereux, and T. W. Ebbesen, “Surface plasmon subwavelength optics,” *nature*, vol. 424, no. 6950, pp. 824–830, 2003.
- [3] W. Feldman, J. Asbridge, S. Bame, M. Montgomery, and S. Gary, “Solar wind electrons,” *Journal of Geophysical Research*, vol. 80, no. 31, pp. 4181–4196, 1975.
- [4] W. Feldman, R. Anderson, S. Bame, S. Gary, J. Gosling, D. McComas, M. Thomsen, G. Paschmann, and M. Hoppe, “Electron velocity distributions near the earth’s bow shock,” *Journal of Geophysical Research: Space Physics*, vol. 88, no. A1, pp. 96–110, 1983.
- [5] T. Ditmire, E. Springate, J. Tisch, Y. Shao, M. Mason, N. Hay, J. Marangos, and M. Hutchinson, “Explosion of atomic clusters heated by high-intensity femtosecond laser pulses,” *Physical Review A*, vol. 57, no. 1, p. 369, 1998.
- [6] J. T. Gudmundsson, J. Alami, and U. Helmersson, “Spatial and temporal behavior of the plasma parameters in a pulsed magnetron discharge,” *Surface and Coatings Technology*, vol. 161, no. 2-3, pp. 249–256, 2002.
- [7] T. J. Armstrong R.J., Weber W.J., “,” *Phys. Lett.*, vol. 74A, pp. 319–322, 1979.
- [8] B. Kadomtsev and O. Pogutse, “Trapped particles in toroidal magnetic systems,” *Nuclear Fusion*, vol. 11, no. 1, p. 67, 1971.
- [9] D. Henry and J. Trguier, “Propagation of electronic longitudinal modes in a non-maxwellian plasma,” *Journal of Plasma Physics*, vol. 8, no. 3, pp. 311–319, 1972.
- [10] E. Saberian and A. Esfandyari-Kalejahi, “Kinetic theory of acoustic-like modes in nonextensive pair plasmas,” *Astrophysics and Space Science*, vol. 349, no. 2, pp. 799–811, 2014.
- [11] A. S. Bains, M. Tribeche, and T. S. Gill, “Modulational instability of electron-acoustic waves in a plasma with a q-nonextensive electron velocity distribution,” *Physics Letters A*, vol. 375, no. 20, pp. 2059–2063, 2011.
- [12] S. Sultana and I. Kourakis, “Electrostatic solitary waves in the presence of excess superthermal electrons: modulational instability and envelope soliton modes,” *Plasma Physics and Controlled Fusion*, vol. 53, no. 4, p. 045003, 2011.
- [13] I. Kourakis and P. K. Shukla, “Electron-acoustic plasma waves: oblique modulation and envelope solitons,” *Physical Review E*, vol. 69, no. 3, p. 036411, 2004.
- [14] S. Singh and G. Lakhina, “Generation of electron-acoustic waves in the magnetosphere,” *Planetary and Space Science*, vol. 49, no. 1, pp. 107–114, 2001.
- [15] R. Ergun, C. Carlson, J. McFadden, F. Mozer, L. Muschietti, I. Roth, and R. Strangeway, “Debye-scale plasma structures associated with magnetic-field-aligned electric fields,” *Physical Review Letters*, vol. 81, no. 4, p. 826, 1998.
- [16] R. Ergun, C. Carlson, J. McFadden, F. Mozer, G. Delory, W. Peria, C. Chaston, M. Temerin, I. Roth, L. Muschietti *et al.*, “Fast satellite observations of large-amplitude solitary structures,” *Geophysical Research Letters*, vol. 25, no. 12, pp. 2041–2044, 1998.
- [17] G. Delory, R. Ergun, C. Carlson, L. Muschietti, C. Chaston, W. Peria, J. McFadden, and R. Strangeway, “Fast observations of electron distributions within auroral source regions,” *Geophysical research letters*, vol. 25, no. 12, pp. 2069–2072, 1998.
- [18] R. Pottellette, R. Ergun, R. Treumann, M. Berthomier, C. Carlson, J. McFadden, and I. Roth, “Modulated electron-acoustic waves in auroral density cavities: Fast observations,” *Geophysical Research Letters*, vol. 26, no. 16, pp. 2629–2632, 1999.
- [19] H. Matsumoto, H. Kojima, T. Miyatake, Y. Omura, M. Okada, I. Nagano, and M. Tsutsui, “Electrostatic solitary waves (esw) in the magnetotail: Ben wave forms observed by geotail,” *Geophysical Research Letters*, vol. 21, no. 25, pp. 2915–2918, 1994.
- [20] J. R. Franz, P. M. Kintner, and J. S. Pickett, “Polar observations of coherent electric field structures,” *Geophysical research letters*, vol. 25, no. 8, pp. 1277–1280, 1998.
- [21] C. Cattell, C. Neiman, J. Dombeck, J. Crumley, J. Wygant, C. Kletzing, W. Peterson, F. Mozer, and M. Andre, “Large amplitude solitary waves in and near the earth’s magnetosphere, magnetopause and bow shock: Polar and cluster observations,” ., 2003.
- [22] P. Shukla and B. Eliasson, “Formation and dynamics of dark solitons and vortices in quantum electron plasmas,” *Physical review letters*, vol. 96, no. 24, p. 245001, 2006.
- [23] B. Sahu and R. Roychoudhury, “Electron acoustic solitons in a relativistic plasma with

- nonthermal electrons,” *Physics of plasmas*, vol. 13, no. 7, p. 072302, 2006.
- [24] P. Shukla and S. Ali, “Dust acoustic waves in quantum plasmas,” *Physics of plasmas*, vol. 12, no. 11, p. 114502, 2005.
- [25] G. Manfredi, “How to model quantum plasmas,” *Fields Inst. Commun.*, vol. 46, pp. 263–287, 2005.
- [26] F. Haas, L. Garcia, J. Goedert, and G. Manfredi, “Quantum ion-acoustic waves,” *Physics of Plasmas*, vol. 10, no. 10, pp. 3858–3866, 2003.
- [27] A. Mamun and P. Shukla, “Solitary waves in an ultrarelativistic degenerate dense plasma,” *Physics of Plasmas*, vol. 17, no. 10, p. 104504, 2010.
- [28] S. Chandra, S. N. Paul, and B. Ghosh, “Electron-acoustic solitary waves in a relativistically degenerate quantum plasma with two-temperature electrons,” *Astrophysics and Space Science*, vol. 343, no. 1, pp. 213–219, 2013.
- [29] S. Chandra and B. Ghosh, “Modulational instability of electron-acoustic waves in relativistically degenerate quantum plasma,” *Astrophysics and Space Science*, vol. 342, no. 2, pp. 417–424, 2012.
- [30] Alireza Abdikian, Jhama Tamang, and Asit Saha. Electron-acoustic supernonlinear waves and their multistability in the framework of the nonlinear schrödinger equation. *Communications in Theoretical Physics*, 72(7):075502, 2020.

Received: 21nd November 2020

Accepted: 22nd December 2020